

Multichannel spectral mode of the ALOHA up-conversion interferometer

L. Lehmann¹, P. Darré^{1,2}, H. Boulogne^{1,3}, L. Delage¹, L. Grossard¹, F. Reynaud¹★

¹Univ. Limoges, CNRS, XLIM, UMR 7252, F-87000 Limoges, France.

²Current address: European Southern Observatory, Karl-Schwarzschild-Str. 2, Garching bei München, 85748, Germany

³Current address: LEUKOS, 37 rue Henri Giffard Z.I. Nord 87280 Limoges

Accepted XXX. Received YYY; in original form ZZZ

ABSTRACT

In this paper, we propose a multichannel spectral configuration of the Astronomical Light Optical Hybrid Analysis (ALOHA) instrument dedicated to high resolution imaging. A frequency conversion process is implemented in each arm of an interferometer to transfer the astronomical light to a shorter wavelength domain. Exploiting the spectral selectivity of this non-linear optical process, we propose to use a set of independent pump lasers in order to simultaneously study multiple spectral channels. This principle is experimentally demonstrated with a dual-channel configuration as a proof-of-principle.

Key words: Instrumentation: high angular resolution – techniques: interferometric.

1 INTRODUCTION

Astronomical Light Optical Hybrid Analysis (ALOHA) is a breakthrough concept for the high angular resolution imaging in astronomy. A general drawing of ALOHA involving two telescopes is shown in Fig 1. Its key idea is to convert infrared astronomical light to shorter wavelength through a process called sum-frequency generation (SFG) (Boyd 1990). This innovative concept takes advantage of non-linear optics and optical fibres to propose a new instrument design compliant with long-baseline interferometer dedicated to the mid-infrared. Intrinsically, ALOHA performs a low flux measurement at room temperature with a narrow spectral selection resulting from the non-linear process.

Convincing preliminary results have been obtained in laboratory with a blackbody source (Gomes et al. 2014), and recently on the sky (Darré et al. 2016) through a collaboration with the CHARA Array team (ten Brummelaar et al. 2005). These studies have been performed in the H astronomical band to take advantage of the mature technology dedicated to optical telecommunications. The frequency conversion is achieved with non-linear crystals that shift H band light to the visible spectral range around 630 nm through SFG.

More recently, ALOHA has been implemented in the L band with preliminary results in the high flux (Szemendera et al. 2016) and in the photon counting regime with a monochromatic source (Szemendera et al. 2017). Over all these studies, the operating conditions of the non-linear process result in an intrinsic spectral selectivity without the addition of any spectrograph. This property has led us to develop a set of experiments with a multiline laser source

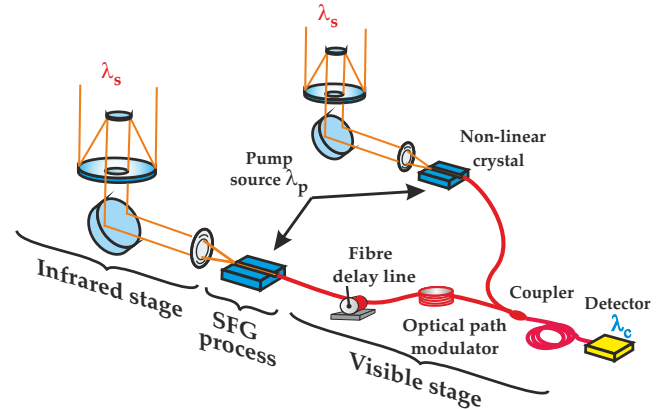


Figure 1. Scheme of the ALOHA interferometer with two telescopes. Powered by a pump source (λ_p), the infrared wavelength (λ_s) coming from the stellar object is up-converted to the wavelength (λ_c) by a sum frequency generation (SFG) process in a non-linear crystal.

used as a pump source in order to broaden the operating spectral span and investigate coherence behaviours of up-conversion detectors. In the first study (Gomes et al. 2013) the science signal included two laser lines and allowed the first demonstration of the spectral compression effect. Two years later, Darré et al. (2015) reported a dual channel spectral configuration using a broadband source. The global interferometric signal resulted from the incoherent superposition of the converted spectral channels but without any possibility of discriminating them.

In this paper, we propose a multichannel spectral mode of

★ e-mail: francois.reynaud@unilim.fr

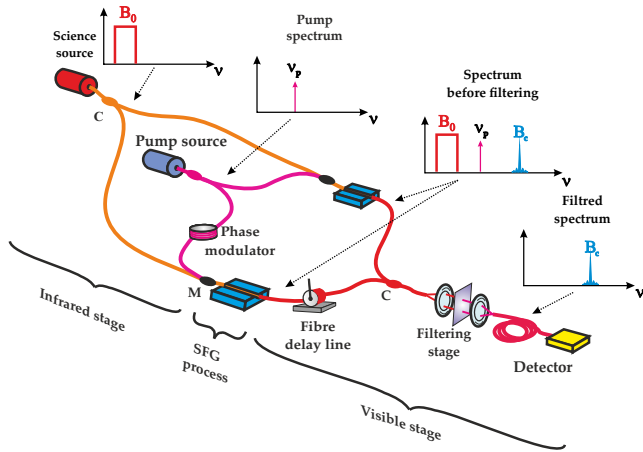


Figure 2. Schematic drawing of a single line laser pump up-conversion interferometer. The broadband science source is mixed with a single line (ν_p) laser pump source by the wavelength division multiplexer (M) in each interferometric arm. The two converted beams are mixed through a fibre coupler (C) to generate the interferometric signal to be detected. At the output of the mixing stage, a filter set allows us to extract the signal of interest from the parasitic ones.

ALOHA, exploiting the spectral selectivity of the non-linear process, in order to simultaneously study several spectral channels. This new configuration is based on a set of independent pump lasers to power the non-linear effects, combined with temporal modulations encoding each converted spectral channel. Thanks to specific differential phase modulations applied on each pump line (made straightforward by the coaxial recombination of the fields), the process does not need any additional component on the astronomical optical paths.

The principle of ALOHA operated with a single line pump source is recalled in section 2. A detailed analysis of the differential spectral phase allows us to predict the interferometric behaviour. In section 3, we develop the multichannel configuration of ALOHA where the non-linear crystals are powered by multiple laser lines as a pump source. In section 4, this principle is experimentally demonstrated in-lab with a two-line pump source configuration.

2 PRINCIPLE OF THE UP-CONVERSION INTERFEROMETER OPERATED WITH A SINGLE LINE PUMP LASER

Figure 2 shows the general principle of a two-arm SFG interferometer as implemented in laboratory and operated with a single laser pump. All the guided components are single mode and polarisation maintaining at the working wavelength. In this test configuration, the two telescopes are replaced by a science source connected to a coupler. The interferometer being fed by a point-like source, the fringe visibility due to the object angular intensity distribution is equal to 1. Therefore the object visibility will not be taken into consideration in the following analysis. The infrared stage carries the beams from the science source (H band) to the non-linear stages through optical fibres. The fibre length imbalance between the two arms leads to a steady differential spectral phase denoted ϕ_s :

$$\phi_s = a_s + b_s \nu_s, \quad (1)$$

where a_s and b_s are the zeroth- and first-order coefficients of this Taylor expansion and ν_s is the frequency of the signal. The energy conservation of the SFG process ($\nu_s = \nu_c - \nu_p$) implies:

$$\phi_s = a_s + b_s(\nu_c - \nu_p), \quad (2)$$

where ν_p and ν_c are respectively the frequency of the pump and the converted light. Due to the narrow operating bandwidth of the non-linear crystals, higher order terms of the spectral phase are not taken into account.

An optical fibre coupler shares the quasi-monochromatic pump source between the two non-linear stages. An optical path modulator installed on one of the pump paths generates a temporal differential phase $\phi_{mod_p} = 2\pi ft$ at a frequency f between the two interferometric arms.

The science and pump waves are merged through a dedicated multiplexer to reach the input of the non-linear conversion stage where the SFG process is operated. This second order non-linear effect generates a converted field with a frequency and phase equal to the sum of the frequencies and phases of the incoming beams (science and pump signals) (DelRio et al. 2008). At the SFG stage outputs, the converted beams are coupled into single mode fibres at ν_c . The fibre length difference between the two interferometric arms leads to a steady differential spectral phase shift ϕ_c :

$$\phi_c = a_c + b_c \nu_c, \quad (3)$$

where a_c and b_c are the coefficient of the Taylor expansion of the static spectral phase in the visible stage.

In addition, an optical fibre delay line implemented on one arm induces a differential phase ϕ_{DL} in order to cancel the group delay in the whole interferometer. This phase ϕ_{DL} can be expressed as a function of the delay line optical path variation δ_c according to the equation:

$$\phi_{DL} = \frac{2\pi\delta_c\nu_c}{c}. \quad (4)$$

The interferometric mixing is achieved by a fibre coupler. In the filtering stage, a set of filters extracts the converted signal from parasitic fields such as pump residues and pump frequency doubling. The global spectral phase difference ϕ between the two arms of the setup is the sum of the contributions over the different stages of the interferometer:

$$\phi = \phi_s + \phi_{mod_p} + \phi_c + \phi_{DL}. \quad (5)$$

Through the non-linear stage, the pump line operates a spectral sampling in the infrared input signal, as shown in Fig. 3. The colormap represents the non-linear conversion efficiency η as a function of ν_s and ν_p . $B_s(\nu_s)$ denotes the sample of the science spectrum density $B_0(\nu_s)$ converted by the pump line at ν_p :

$$B_s(\nu_s) = B_0(\nu_s) \cdot \eta(\nu_s, \nu_p). \quad (6)$$

The related power spectral density of the converted signal $B_c(\nu_c)$ corresponds to $B_s(\nu_s)$ shifted by the pump line through the non-linear process.

$$B_c(\nu_c) = B_s(\nu_s) * \delta(\nu_p), \quad (7)$$

where $*$ denotes the convolution product.

To preserve the mutual coherence of the fields in the interferometer, care has to be taken to precisely overlap the spectral acceptances of each interferometric arm when the two non-linear crystals are powered by the same pump line at ν_p . This fine overlapping is achieved by an accurate thermal servo control of the non-linear crystals. Assuming this condition is satisfied, the interferometric

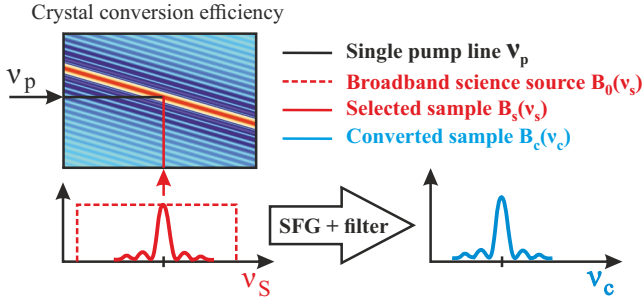


Figure 3. Scheme illustrating the spectral sampling effect operated by the SFG process. The colormap shows the conversion efficiency $\eta(v_s, v_p)$ as a function of the pump frequency v_p (vertical axis) and the science frequency v_s (horizontal axis). The low to high conversion efficiency is displayed from blue to red. Due to its narrow band, the pump signal at v_p samples (horizontal section) the broadband science source spectrum $B_0(v_s)$ and generates the related converted signal spectrum $B_c(v_c)$.

Table 1. Phase contribution summary of the different optical stages.

Stage	Phase delay	Group delay
Infrared stage (ϕ_s)	$a_s - b_s v_p$	$b_s v_c$
Pump stage	ϕ_{mod_p}	-
Converted stage (ϕ_c)	a_c	$b_c v_c$
Delay line (ϕ_{DL})	-	$(2\pi\delta_c v_c)/c$

signal related to an elementary spectral contribution at v_c can be written as:

$$dI(v_c) = B_c(v_c)[1 + \cos(\phi)]dv_c, \quad (8)$$

The global interferometric signal can be derived by integrating dI over the converted frequency v_c :

$$I = \int B_c(v_c)[1 + \cos(\phi)]dv_c. \quad (9)$$

Table 1 summarises the phase contributions of the different optical stages. It is possible to cancel the group delay in the interferometer (right column of Table 1) by adjusting the delay line group delay δ_c such as:

$$\phi_{DL} = -(b_s + b_c)v_c. \quad (10)$$

In such experimental conditions, ϕ no longer depends on v_c :

$$\phi = a_s + a_c - b_s v_p + \phi_{mod_p} = \phi_0 + \phi_{mod_p}, \quad (11)$$

with ϕ_0 a constant phase term. In this way, the interferometric signal defined by equation 9 can be expressed as:

$$I = (1 + \cos(\phi)) \int B_c(v_c)dv_c. \quad (12)$$

$\int B_c(v_c)dv_c$ corresponds to the total power, denoted P , of the spectral sample selected through the non-linear process. As the spectral resolution is defined by the related spectral acceptance Δv_s , preserved through the SFG process, we can write:

$$P = \int B_c(v_c)dv_c = \int \eta(v_s, v_p)B_s(v_s)dv_s. \quad (13)$$

In the case of a science source with a flat spectrum within Δv_s , P can be approximated by:

$$P = B_0(v_{s0}) \int \eta(v_s, v_p)dv_s = B_0(v_{s0})\eta_0\Delta v_s, \quad (14)$$

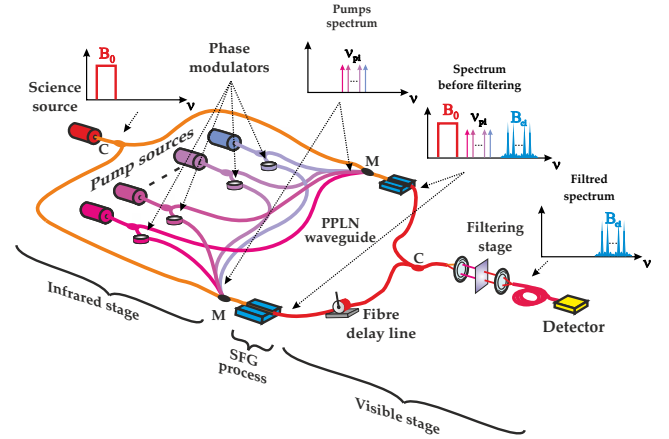


Figure 4. Up-conversion interferometer in multichannel mode. Each pump wave is phase-modulated on the first arm of the interferometer.

where v_{s0} is the central frequency of the conversion efficiency $\eta(v_s, v_p)$ and η_0 the maximum conversion efficiency.

This spectrum sample then is tagged at the frequency f by the temporal modulation of the pump phase ϕ_{mod_p} . The interferometric signal can be expressed as:

$$I(t) = P \cdot [1 + \cos(2\pi ft + \phi_0)]. \quad (15)$$

In the next section, we describe an interferometric configuration that processes several spectral samples simultaneously in order to operate ALOHA in a multichannel mode.

3 PRINCIPLE OF THE UP-CONVERSION INTERFEROMETER OPERATED IN MULTICHANNEL SPECTRAL MODE

Figure 4 shows the general principle of a two arm up-conversion interferometer operating in multichannel mode. The infrared and converted stages are unchanged, leading to identical expressions for ϕ_s , ϕ_{DL} and ϕ_c as defined in section 2. Conversely, the pump stage is significantly modified. A set of pump lines is provided by a pump laser assembly. Each pump laser i is quasi-monochromatic and emits a frequency v_{pi} . Optical fibre couplers allow us to share the pump sources between the two interferometric arms and optical path modulators induce a specific phase difference $\phi_{mod_{pi}} = 2\pi f_i t$ at a frequency f_i on the pump i . This individual control of each pump phase is the key improvement compared with our previous work (Darré et al. 2015) and enables the spectral channel discrimination.

Each pump line at frequency v_{pi} converts a spectral sample i according to the non-linear crystal properties.

$$B_{si}(v_s) = B_0(v_s) \cdot \eta(v_s, v_{pi}). \quad (16)$$

The related spectral density of the converted signal $B_{ci}(v_c)$ is equal to the infrared signal spectrum $B_{si}(v_s)$ shifted by v_{pi} through the non-linear process as shown in Fig. 5:

$$B_{ci}(v_c) = B_{si}(v_s) * \delta(v_{pi}). \quad (17)$$

Assuming a fine overlapping of the two converted spectra, the interferometric signal related to each pump line v_{pi} can be derived as:

$$dI_i = B_{ci}(v_c)[1 + \cos(\phi_i)]dv_c. \quad (18)$$

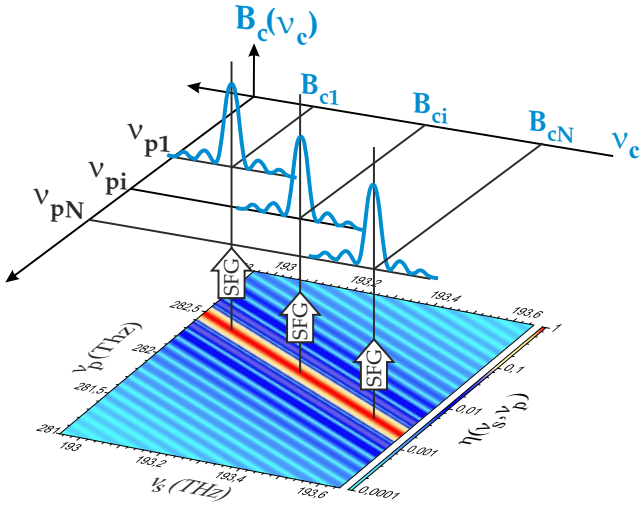


Figure 5. Converted signal spectrum $B_{ci}(v_c)$ corresponding to the spectrum $B_{si}(v_c)$ selected by the pump frequency v_{pi} . The maximum of conversion efficiency $\eta(v_s, v_p)$ of the crystal is shown in red on the colormap.

The global interferometric contributions for the spectral sample i can be written by integrating dI_i .

$$I_i = \int B_{ci}(v_c)[1 + \cos(\phi_i)]dv_c. \quad (19)$$

By adjusting the delay line position δ_c , it is possible to cancel the group delay in the interferometer so that all the spectral phases ϕ_i no more longer depend on v_c :

$$\phi_i = a_s + a_c - b_s v_{pi} + \phi_{mod_{pi}} = \phi_{0i} + \phi_{mod_{pi}}. \quad (20)$$

with ϕ_{0i} a constant phase term. When operating all the pump lines simultaneously, the total interferometric signal is the incoherent superposition of all the I_i contributions:

$$I = \sum_i I_i = \sum_i \left[(1 + \cos(\phi_i)) \int B_{ci}(v_c)dv_c \right]. \quad (21)$$

According to equation 13, we define the power P_i for each spectral sample as following:

$$P_i = \int B_{ci}(v_c)dv_c = \int \eta(v_s, v_{pi})B_{si}(v_s)dv_s. \quad (22)$$

As in the single pump case, assuming that the science source has a flat spectrum within each spectral acceptance Δv_s , P_i can be expressed as:

$$P_i = B_0(v_{si}) \int \eta(v_s, v_{pi})dv_s = B_0(v_{si})\eta_0\Delta v_s, \quad (23)$$

where v_{si} is the central frequency of each conversion efficiency $\eta(v_s, v_{pi})$ and η_0 the maximum conversion efficiency.

The appropriate temporal modulation of $\phi_{mod_{pi}}$ tags each spectral channel at the interferometric signal frequency f_i through the modulation term $\cos(\phi_i)$.

The global interferometric signal can be expressed as:

$$I(t) = \sum_i P_i [1 + \cos(2\pi f_i t + \phi_{0i})]. \quad (24)$$

As shown in Fig. 6, those frequencies f_i are generated by the pump phase modulation driven by dedicated linear slopes. Using a specific fringe modulation frequency f_i for each spectral sample i allows

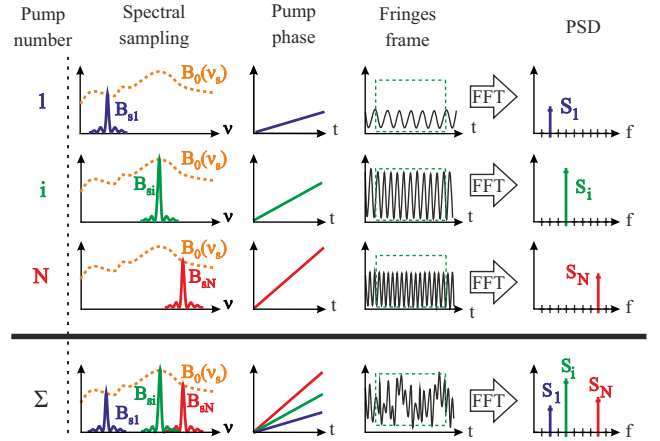


Figure 6. Effect of the pump phase modulation in multichannel mode. Each pump associated to a spectral sample i (for $i = 1$ to N) of the source spectrum $B_0(v_s)$ is linearly modulated. The amplitude of this modulation is different for each pump and tags the corresponding fringes with a dedicated frequency f_i . Frames of fringes are then demodulated with a Fast Fourier Transform (FFT). The fringe peaks S_i in the Power Spectrum Density (PSD) show the contribution of the different spectral samples.

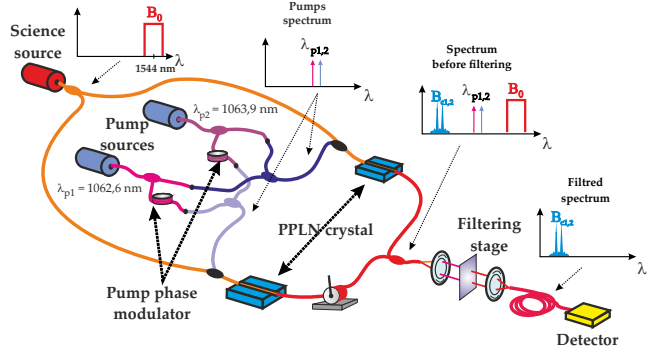


Figure 7. General scheme of our experimental interferometer setup. The internal source is multiplexed with two modulated pump signals. The nonlinear crystals operate the SFG process in order to shift the infrared samples to the visible ones. The two arms of the interferometer are then mixed to produce fringes. The detector is a silicon avalanche photodiode.

us to perform a spectral analysis by a simple Fourier transform of the interferometric output signal. It is important to note that no additional component is necessary on the science channel to switch from the single pump mode to the multichannel one. The only change is applied on the pump source stage and on the related differential phase modulations. In addition, the position of the fringe peaks S_i can be reordered at convenience in the Fourier transform of the interferometric signal by choosing a specific set of modulation frequencies f_i .

Using this configuration in a telescope array, it could be possible to measure most of the classic interferometric observables: absolute visibility, differential visibility, differential phase and closure phase. The detailed data processing is however beyond the scope of this article.

Table 2. Overview of the wavelengths involved in the SFG processes. λ_s : signal, λ_p : pump, and λ_c : converted.

Sample	λ_s	λ_p	λ_c
1	1554.0 nm	1062.6 nm	631.08 nm
2	1551.6 nm	1063.9 nm	631.14 nm

4 EXPERIMENTAL DEMONSTRATION

The multichannel spectral mode of ALOHA has been experimentally demonstrated with the fibre Mach-Zehnder interferometer shown in Fig. 7. This setup comprises four main elements: the signal source, the pump laser assembly, the SFG process stage, and finally the recombination, filtering and detection modules. All over the interferometric arms, the optical fibres are single mode and polarisation maintaining at the operating wavelength.

The science signal is provided by a superluminescent source (SLED) in the mW power range. Its spectrum is centred at 1544 nm and spreads over a 40 nm bandwidth (FWHM). This signal is split through a coupler toward the two interferometric arms. Our experimental demonstration uses only two pumps for the sake of simplicity and cost considerations. We use independent amplified distributed feedback lasers set at a steady wavelength during the whole experiment: $\lambda_{p1} = 1062.6$ nm for pump 1 and $\lambda_{p2} = 1063.9$ nm for pump 2. For each pump source, the signal is divided by a 1×2 coupler. One of the fibre outputs is coiled around a cylindrical piezoelectric actuator to perform the $\phi_{mod_{pi}}$ phase modulation.

The signal and pump beams are merged by multiplexers implemented at the input of each conversion stage. The frequency conversion is achieved through a Periodically Poled Lithium Niobate (PPLN) waveguide provided by the NTT corporation. It is based on a ridge technology with a fibre pigtail at both ends. Its length is 2.2 cm and the conversion efficiency has a $\Delta\lambda = 0.6$ nm bandwidth centred near 1550 nm (depends on the pump wavelength, see Table 2). According to the quasiphase matching condition, each pump line converts a sample of the broadband source.

The outputs of the two conversion stages are mixed with a 2×1 coupler in order to generate the interferometric fringes of the converted signal. The filtering stage rejects the residual light of pump. For this purpose, a set of band-pass filters centred around the converted wavelength $\lambda_c = 630$ nm is used. The output signal of the SFG interferometer is detected by a silicon avalanche photodiode. As a result of the temporal phase modulation $\phi_{mod_{pi}}$ applied on the pump source stage, the interferometric signal is displayed as a function of time. For each measurement, an analogue-to-digital converter records frames of 0.2 s duration. Over the frame duration, the amplitude voltage applied on each pump piezoelectric actuator evolves linearly as a function of time.

The appropriate amplitude is applied on the optical path modulator of the first channel to get 22 fringes per frame. The interferometric signal is then digitally processed by a Fast Fourier Transform (FFT) to extract the Power Spectral Density (PSD). It results in a peak S_1 at the 22nd digital channel related to the spectral sample 1 as shown in Fig. 8. At the same time, the second spectral sample phase modulation slope is set to observe 24, 26, 28, 30 or 32 fringes per frame. The related peak S_2 in the PSD curve at the spectral channel 24, 26, 28, 30 or 32 corresponds to the spectral sample 2. These experimental results demonstrate spectroscopic functionality and the ability of ALOHA to process simultaneously two spectral samples and to display them at will. This versatility could be very helpful to reorganise the spectrum processing for differential measurements.

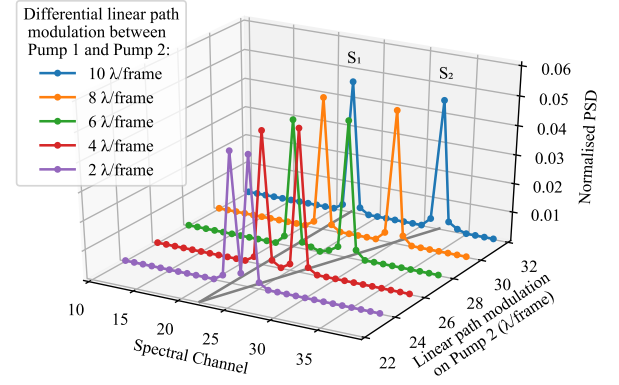


Figure 8. Experimental measurements of the converted interferometric signal normalised PSD. Each curve corresponds to a specific difference in the amplitude of the path modulation applied between pump 1 and pump 2.

5 CONCLUSIONS

We have experimentally demonstrated the ability of the ALOHA instrument to work in a multichannel spectral mode. Each converted sample of a science source spectrum can be tagged through the temporal encoding of the pump differential phases. We used two pump lines to achieve this new operating mode of ALOHA in a laboratory experiment. Further work can now be done in order to take full advantage of a multichannel mode. A much complex pump laser assembly can be set in order to get broadband spectral information of a science source. This work has been done in the H band but can be directly transposed to an up-conversion interferometer in the L band.

ACKNOWLEDGMENTS

This work has been financially supported by the Institut National des Sciences de l'Univers (INSU), the Centre National d'Études Spatiales (CNES) and Thales Alenia Space. Our thanks go also to A. Dexte for the development and his advice for all the specific mechanical components.

REFERENCES

- Boyd R. W., 1990, *Nonlinear Optics*, 3rd edn. Academic Press, New York, USA
- Darré P., Szemendera L., Grossard L., Delage L., Reynaud F., 2015, *Opt. Express*, 23, 25450
- Darré P., et al., 2016, *Phys. Rev. Lett.*, 117, 233902
- DelRio L., Ribiere M., Delage L., Reynaud F., 2008, *Optics Communications*, 281, 2722
- Gomes J.-T., Grossard L., Ceus D., Vergnole S., Delage L., Reynaud F., Herrmann H., Sohler W., 2013, *Opt. Express*, 21, 3073
- Gomes J.-T., et al., 2014, *Physical Review Letters*, 112, 143904
- Szemendera L., Darré P., Baudoin R., Grossard L., Delage L., Herrmann H., Silberhorn C., Reynaud F., 2016, *Monthly Notices of the Royal Astronomical Society*, 457, 3115
- Szemendera L., Grossard L., Delage L., Reynaud F., 2017, *J. 10.1093/mnras/stx780*, 468, 3484
- ten Brummelaar T. A., et al., 2005, *The Astrophysical Journal*, 628, 453

This paper has been typeset from a \TeX/L\AA\TeX file prepared by the author.